inorganics

MDPI

Article

CO_2@C_{84}: DFT Calculations of Structure and Energetics

Zdeněk Slanina [1,2,*], Filip Uhlík [3], Takeshi Akasaka [2], Xing Lu [2] and Ludwik Adamowicz [1]

[1] Department of Chemistry and Biochemistry, University of Arizona, Tucson, AZ 85721-0041, USA
[2] State Key Laboratory of Materials Processing and Die & Mould Technology, School of Material, Science and Engineering, Huazhong University of Science and Technology, Wuhan 430074, China
[3] Department of Physical and Macromolecular Chemistry, Faculty of Science, Charles University, Albertov 6, 128 43 Praha 2, Czech Republic
* Correspondence: zdeneks@email.arizona.edu

Abstract: Encapsulations of carbon dioxide into D_2(22)-C_{84} and D_{2d}(23)-C_{84} fullerenes are evaluated. The encapsulation energy is computed with the DFT M06-2X/6-31+G* approach corrected for the basis set superposition error evaluated by the counterpoise method. The resulting encapsulation energy for CO_2@D_2(22)-C_{84} and CO_2@D_{2d}(23)-C_{84} amounts to substantial values of −14.5 and −13.9 kcal/mol, respectively. The energy gain is slightly larger than for CO@C_{60}, already synthesized with a high-temperature and high-pressure treatment—so that a similar preparation of CO_2@C_{84} could be possible. The calculated rotational constants and IR vibrational spectra are presented for possible use in detection. The stability of $(CO_2)_2$@C_{84} is also briefly discussed.

Keywords: metallic and non-metallic endohedrals; fullerene encapsulation; stability calculations; theory–experiment comparison

1. Introduction

Interactions of carbon dioxide with fullerenes have been studied [1–3], for example, for boron-based fullerene cage B_{80} [1]. Interestingly, additions of endohedral fullerenes [4,5] or carbon dioxide [6] can improve the efficiency of solar cells. Various non-metallic molecules can also be encapsulated inside fullerene cages. N_2@C_{60} and N_2@C_{70} were the first such non-metal endohedrals, namely prepared [7] by heating under high pressure and with a catalyst. Moreover, there is also an elegant synthetic technique that first places molecules inside open fullerene cages and then the cages are synthetically closed—for example, the preparation [8] of $(H_2O)_2$@C_{70}.

Such fullerene encapsulations of non-metals have also been calculated, e.g., in [9–14]. The first such calculations [9] from the year 1991 treated small molecules (H_2, N_2, CO, and LiH) trapped inside the C_{60} cage and predicted a blue shift in the stretching frequencies. Later on, encapsulations of larger non-metal molecules into fullerene cages were also calculated [10–14], for example, MH_4 hydrides [10] or water molecules [11,14]. Moreover, the endohedral CH_4@C_{60} was synthesized recently [12], and its stabilization energy was calculated [13] as −13.5 kcal/mol.

As CO@C_{60} could also be prepared [7] by the high-temperature and high-pressure treatment, there is a question regarding if CO_2 may also be encapsulated in some (larger) fullerene cages. In this report, the issue is calculated for the first time—namely for the two lowest-energy and most common C_{84} fullerenes D_2(22)-C_{84} and D_{2d}(23)-C_{84} [15]. The pristine D_2 and D_{2d} C_{84} isomers are produced via high-temperature synthesis [15,16] in a ratio of 2:1. The D_{2d} structure is located [17] only about 0.5 kcal/mol below the

check for updates

Academic Editor: Ben McLean

Received: 30 November 2024
Revised: 9 January 2025
Accepted: 11 January 2025
Published: 14 January 2025

Citation: Slanina, Z.; Uhlík, F.; Akasaka, T.; Lu, X.; Adamowicz, L. CO_2@C_{84}: DFT Calculations of Structure and Energetics. *Inorganics* **2025**, *13*, 19. https://doi.org/10.3390/inorganics13010019

D_2 species. However, the chirality factor also contributes [15] to the D_2/D_{2d} relative isomeric populations.

2. Calculations

The calculations are carried out with density-functional theory (DFT) treatment, namely using the DFT M06-2X functional comprehensively tested [18] for thermochemistry, kinetics, noncovalent interactions, and other applications. The M06-2X functional is employed with the standard 6-31+G* basis set [19] (M06-2X/6-31+G* approach). The geometry optimizations are performed with the analytical first derivatives of energy. In the localized stationary points, the harmonic vibrational GF analysis is carried out using the analytical second derivatives of energy. The vibrational analysis can confirm that energy minima were indeed localized. For DFT integration, the so-called ultrafine grid is applied (and then refined with the superfine grid). For the SCF (self-consistent field) convergence, the tight criterion is used. The wavefunction stability is systematically tested in order to avoid unphysical unstable SCF solutions.

The encapsulation energy [20] is corrected for the so-called basis set superposition error (BSSE) evaluated by the approximative Boys–Bernardi counterpoise method [21] (also labeled [22] CP2). The counterpoise method guarantees that every component of a treated chemical reaction is formally described by the same number of basis-set functions so that their total energies are comparable. The BSSE correction term constitutes an important refinement of the encapsulation energy. Without the BSSE correction, the energy gain produced by encapsulation process would be overestimated (i.e., products would be overstabilized).

The reported computations are carried out with the Gaussian program package [22]. The calculations are performed on computers operating in parallel regime, mostly with 8–24 processors (computational frequency up 3 GHz each; available operational memory up to 60 GB).

3. Results and Discussion

The calculated encapsulation energy ΔE_{enc} means the potential-energy change along the studied gas-phase association process, for example for encapsulation in the $D_2(22)$-C_{84} fullerene cage:

$$CO_2(g) + D_2(22) - C_{84}(g) = CO_2@D_2(22) - C_{84}(g), \quad (1)$$

and similarly for the $D_{2d}(23)$-C_{84} cage. The M06-2X/6-31+G*-calculated encapsulation energy values with and without the BSSE correction are presented in Table 1.

Table 1. The calculated encapsulation energy ΔE_{enc} for $CO_2@D_2(22)$-C_{84} [a] and $CO_2@D_{2d}(23)$-C_{84} [b].

Species	Level	ΔE_{enc} (kcal/mol) No BSSE	BSSE
$CO_2@D_2(22)$-C_{84}	M06-2X/6-31G*	−16.4	−12.1
$CO_2@D_2(22)$-C_{84}	M06-2X/6-31+G*	−17.7	−14.5
$CO_2@D_{2d}(23)$-C_{84}	M06-2X/6-31G*	−16.2	−11.7
$CO_2@D_{2d}(23)$-C_{84}	M06-2X/6-31+G*	−17.2	−13.9

[a] See Figure 1. [b] See Figure 2.

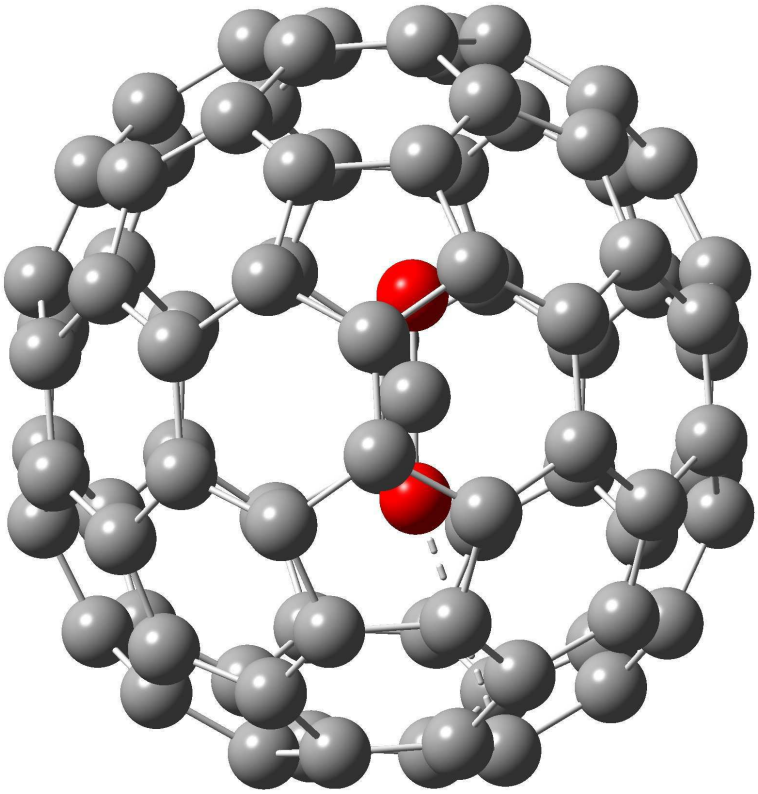

Figure 1. The M06-2X/6-31+G*-optimized structure of CO_2@D_2(22)-C_{84} (the shortest contact of O with the cage carbon is indicated by dashed line).

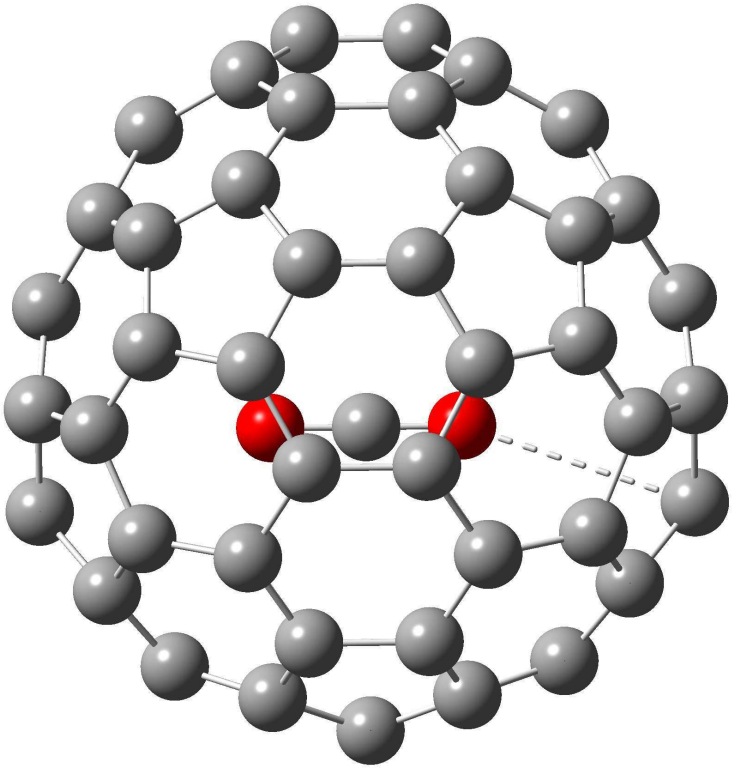

Figure 2. The M06-2X/6-31+G*-optimized structure of CO_2@D_{2d}(23)-C_{84} (the shortest contact of O with the cage carbon is indicated by dashed line).

The BSSE-corrected M06-2X/6-31+G* encapsulation energy ΔE_{enc} for CO_2@D_2(22)-C_{84} and CO_2@D_{2d}(23)-C_{84} amounts to −14.5 and −13.9 kcal/mol, respectively. At this

computational level, the BSSE correction reduces the energy gain owing to the encapsulation by about 3 kcal/mol. For illustrative comparison, the encapsulation energies evaluated with smaller basis sets are also presented, i.e., for the M06-2X/6-31G* computational approach but still in the same M06-2X/6-31+G* optimized structures. As for the smaller basis set, the M06-2X/6-31G* energy gain without the BSSE term is reduced by less than 2 kcal/mol compared to the M06-2X/6-31+G* approach. On the other hand, the BSSE correction provides a larger reduction in energy gain with the smaller basis (the M06-2X/6-31G* approach), namely by about 4 kcal/mol. This finding is in agreement with a general feature of the BSSE correction: the correction term would disappear in a situation of a basis set with an infinite number of basis functions (clearly enough, such an infinite computational scheme cannot practically be handled). Overall, the ΔE_{enc} terms in Table 1 are somewhat more sensitive to the BSSE correction than to the basis-set choice. The calculated gain in encapsulation energy is slightly larger than in the case of $CO@C_{60}$, for which the encapsulation energy is calculated to be [23] about −12.5 kcal/mol. The finding suggests that $CO_2@C_{84}$ could possibly be prepared by the high-temperature and high-pressure treatment [7] too.

Table 2 presents four calculated characteristics of the $CO_2@C_{84}$ endohedrals—the closest contact of oxygen atoms with the cage carbons, the total charge on the C_{84} cages, and the lowest and highest vibrational frequency values. The shortest distance of oxygen to the cage is, in both cases, about 3 Å. There is some small charge transfer from the CO_2 unit to the cage. The Mulliken atomic charges evaluated at the M06-2X/3-21G level show negative charge transfer to the cage of −0.02 (in elementary charge units). Such rather negligible charge transfer stands in clear contrast to the substantial charge donations associated with [14] metallofullerenes. Let us mention that the Mulliken atomic charges, owing to their construction, are to be evaluated with smaller basis sets, for example, the standard 3–21G basis set applied here. The Mulliken atomic charges computed with the 3–21G basis set are known [14] to yield, for endohedral metallofullerenes, fair agreement with the available observed atomic charges [24]. Moreover, there are also deeper computational arguments [25,26] as to why larger basis sets should not be considered for the evaluation of the Mulliken charges on atoms.

Table 2. The selected characteristics of $CO_2@D_2(22)$-C_{84} and $CO_2@D_{2d}(23)$-C_{84}—the closest O-cage contact [a] r_{O-C}, the total charge [b] on cage q_c, the lowest vibrational frequency [a] ω_{low}, and the highest vibrational frequency [a] ω_{high}.

Species	r_{O-C}/Å	q_c	ω_{low}/cm^{-1}	ω_{high}/cm^{-1}
$CO_2@D_2(22)$-C_{84} [c]	3.07	−0.012	12.7	2425
$CO_2@D_{2d}(23)$-C_{84} [d]	3.05	−0.017	37.2	2431

[a] M06-2X/6-31+G* values. [b] M06-2X/3-21G values. [c] See Figure 1. [d] See Figure 2.

The harmonic vibrational analysis is considered here not only for the confirmation that energy minima were indeed found (no imaginary frequency) but also for simulations of the infrared (IR) spectra as they can be used for identification of the $CO_2@C_{84}$ endohedrals when prepared. Figure 3 shows the M06-2X/6-31+G*-calculated IR vibrational spectra for $CO_2@D_2(22)$-C_{84} and $CO_2@D_{2d}(23)$-C_{84}. The lowest vibrational frequency ω_{low} belongs to a rotational motion of CO_2 as a whole within the cage. The free CO_2 molecule has four vibrational modes; their harmonic frequencies at the M06-2X/6-31+G* level are double-degenerated bending mode 670 cm^{-1}, symmetric bond stretching 1411 cm^{-1}, and asymmetric bond stretching 2461 cm^{-1}. After encapsulation, the CO_2 frequencies are somewhat shifted (and the degeneracy removed) owing to the interactions with cages. In the case of $CO_2@D_2(22)$-C_{84}, the M06-2X/6-31+G*-calculated frequencies are 652.2, 652.8, 1404,

and 2425 cm^{-1} (i.e., ω_{high} in Table 2). Similarly, for $CO_2@D_{2d}$-C_{84}, the M06-2X/6-31+G* frequencies are 650.2, 650.4, 1408, and 2431 cm^{-1}. The asymmetric C-O bond stretching is actually the strongest peak in the IR spectra (Figure 3).

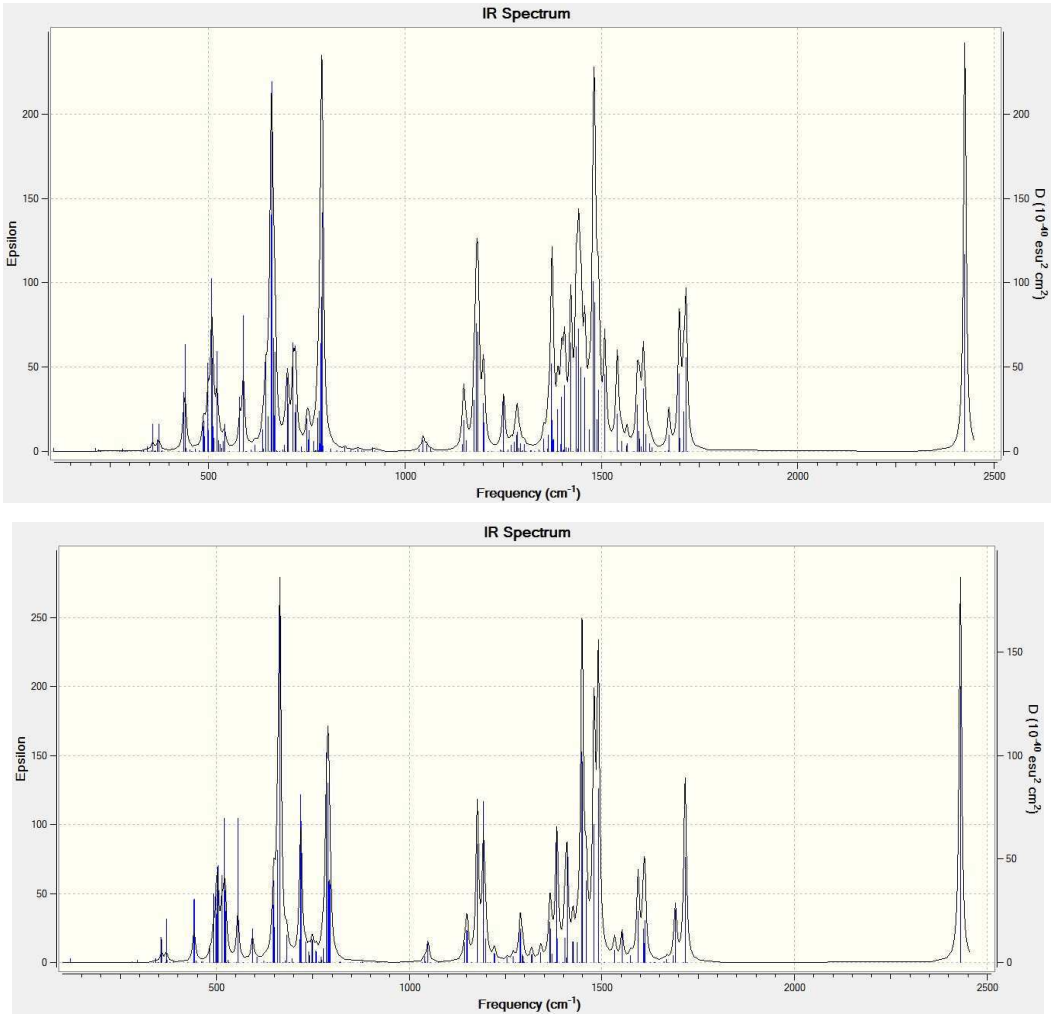

Figure 3. M06-2X/6-31+G*-computed IR spectra of $CO_2@D_2(22)$-C_{84} (**top**) and $CO_2@D_{2d}(23)$-C_{84} (**bottom**) .

Incidentally, the recent final confirmation with electron spectroscopy [27] of the presence of C_{60} in the interstellar space encourages further cosmic searches [28–30]—even for fullerene cages with some encapsulates inside (incidentally, pressure of CO_2 at Venus can reach [31] some 90 atm). As rotational spectroscopy could be used for the detection of fullerene species in interstellar space, Table 3 presents the computed rotational constants, *A*, *B*, and *C*, for the $CO_2@C_{84}$ endohedrals (although, in interstellar space, we can rather expect the species in an ionized form).

Table 3. The M06-2X/6-31+G* rotational constants *A*, *B*, *C* [GHz] of the $CO_2@C_{84}$ endohedrals.

Endohedral [a]	*A*	*B*	*C*
$CO_2@D_2(22)$-C_{84} [a]	0.044112	0.042604	0.041344
$CO_2@D_{2d}(23)$-C_{84} [b]	0.042788	0.042649	0.042555

[a] See Figure 1. [b] See Figure 2.

Similar DFT calculations for related encapsulation in Equation (2), producing $(CO_2)_2$@C_{84}, are now also in progress; for CO_2@$D_2(22)$-C_{84}, they concern the gas-phase process:

$$2CO_2(g) + D_2(22) - C_{84}(g) = (CO_2)_2@D_2(22) - C_{84}(g), \quad (2)$$

and similarly for the $D_{2d}(23)$-C_{84} cage. However, in order to compare the relative reaction populations of the related endohedrals with one and two encapsulated CO_2 molecules, even the encapsulation equilibrium constants $K_{p,enc}(i)$ would be needed. For the process in Equation (1), the first step would be the construction of the encapsulation equilibrium constant $K_{p,enc}(1)$ (defined by the partial pressures p of the individual reaction components):

$$K_{p,enc}(1) = \frac{p_{CO_2@D_2(22)-C_{84}}}{p_{CO_2} p_{D_2(22)-C_{84}}}. \quad (3)$$

Then, the equilibrium constant $K_{p,enc}(2)$ for encapsulation in Equation (2) should also be calculated:

$$K_{p,enc}(2) = \frac{p_{(CO_2)_2@D_2(22)-C_{84}}}{p^2_{CO_2} p_{D_2(22)-C_{84}}}. \quad (4)$$

From Equation (3) and Equation (4), we can obtain the required population ratio of the two endohedrals:

$$\frac{p_{(CO_2)_2@D_2(22)-C_{84}}}{p_{CO_2@D_2(22)-C_{84}}} = p_{CO_2} \frac{K_{p,enc}(2)}{K_{p,enc}(1)}. \quad (5)$$

Equation (5) straightforwardly shows how the CO_2 pressure p_{CO_2} influences the population ratio of $(CO_2)_2$@$D_2(22)$-C_{84} and CO_2@$D_2(22)$-C_{84} endohedrals. The encapsulation equilibrium constants $K_{p,enc}(i)$ can be calculated using molecular partition functions supplied with rotational and vibrational parameters generated by DFT calculations.

4. Conclusions

Calculations are reported for the encapsulation of carbon dioxide into the two most common C_{84} fullerenes, $D_2(22)$-C_{84} and $D_{2d}(23)$-C_{84}, yielding CO_2@$D_2(22)$-C_{84} and CO_2@$D_{2d}(23)$-C_{84}. The calculations are carried out with the DFT M06-2X/6-31+G* approach. The resulting encapsulation energy for CO_2@$D_2(22)$-C_{84} and CO_2@$D_{2d}(23)$-C_{84} amounts to substantial values of −14.5 and −13.9 kcal/mol, respectively. The energy gain is slightly larger than for CO@C_{60}. As CO@C_{60} was already synthesized by heating under high pressure with a catalyst, similar high-temperature and high-pressure preparation of CO_2@C_{84} or even $(CO_2)_2$@C_{84} could be possible. The computational treatment should be expanded in the future by evaluations of the related encapsulation equilibrium constants. The presented results encourage similar computational studies for still more complex [32–36] endohedral and other nanocarbon systems.

Author Contributions: Conceptualization, Z.S., T.A. and X.L.; methodology, Z.S. and L.A.; hardware and software, Z.S., F.U. and L.A.; models validation, Z.S., T.A., X.L. and L.A.; analysis and interpretation, Z.S., F.U., T.A. and X.L.; writing—original draft preparation, Z.S. and F.U. All authors have read and agreed to the published version of the manuscript.

Funding: The reported research has been supported by the National Natural Science Foundation of China (21925104 and 92261204), the Hubei Provincial Natural Science Foundation of China (No. 2021CFA020), and the International Cooperation Key Project of Science and Technology Department of Shaanxi; and by the Charles University Centre of Advanced Materials/CUCAM (CZ.02.1.01/0.0/0.0/15_003/0000417), the MetaCentrum (LM2010005), and CERIT-SC (CZ.1.05/3.2.0-0/08.0144) computing facilities.

Data Availability Statement: The data presented in this study are available in article.

Acknowledgments: A very initial phase of the research line was supported by the Alexander von Humboldt-Stiftung and the Max-Planck-Institut für Chemie (Otto-Hahn-Institut).

Conflicts of Interest: The authors declare no conflict of interest.

References

1. Sun, Q.; Wang, M.; Li, Z.; Du, A.; Searles, D.J. Carbon dioxide capture and gas separation on B_{80} fullerene. *J. Phys. Chem. C* **2014**, *118*, 2170–2177. [CrossRef]
2. Meloni, G.; Giustini, A.; Park1, H. CO_2 activation within a superalkali-doped fullerene. *Front. Chem.* **2021**, *9*, 712960-1–712960-8. [CrossRef]
3. Palakkal, A.S.; Pillai, R.S. Unraveling the role of fullerene encapsulation driven CO_2 capture in square pillared Bio-HOF under humid condition by advanced molecular simulation. *Separ. Purif. Technol.* **2023**, *325*, 124650-1–124650-12. [CrossRef]
4. Ross, R.B.; Cardona, C.M.; Guldi, D.M.; Sankaranarayanan, S.G.; Reese, M.O.; Kopidakis, N.; Peet, J.; Walker, B.; Bazan, G.C.; Van Keuren, E.; et al. Endohedral fullerenes for organic photovoltaic devices. *Nature Mater.* **2009**, *8*, 208–212. [CrossRef]
5. Ye, X.; Yu, P.; Shen, W.; Hu, S.; Akasaka, T.; Lu, X. Er@C_{82} as a bifunctional additive to the spiro-OMeTAD hole transport layer for improving performance and stability of perovskite solar cells. *Sol. RRL* **2021**, *5*, 2100463-1–2100463-9. [CrossRef]
6. Kong, J.; Shin, Y.; Röhr, J.A.; Wang, H.; Meng, J.; Wu, Y.; Katzenberg, A.; Kim, G.; Kim, D.Y.; Li, T.-D.; et al. CO_2 doping of organic interlayers for perovskite solar cells. *Nature* **2021**, *594*, 51–56. [CrossRef]
7. Peres, T.; Cao, B.P.; Cui, W.D.; Khong, A.; Cross, R.J.; Saunders, M.; Lifshitz, C. Some new diatomic molecule containing endohedral fullerenes. *Int. J. Mass Spectr.* **2001**, *210/211*, 241–247. [CrossRef]
8. Zhang, R.; Murata, M.; Aharen, T.; Wakamiya, A.; Shimoaka, T.; Hasegawa, T.; Murata Y. Synthesis of a distinct water dimer inside fullerene C_{70}. *Nature Chem.* **2016**, *8*, 435–441. [CrossRef] [PubMed]
9. Cioslowski, J. Endohedral chemistry: Electronic structures of molecules trapped inside the C_{60} cage. *J. Am. Chem. Soc.* **1991**, *113*, 4139–4141. [CrossRef]
10. Charkin, O.P.; Klimenko, N.M.; Charkin, D.O.; Mebel, A.M. Theoretical study of host-guest interaction in model endohedral fullerenes with tetrahedral molecules and ions of MH4 hydrides inside the $C_{60}H_{36}$, $C_{60}H_{24}$, C_{84}, and C_{60} cages. *Russ. J. Inorg. Chem.* **2004**, *49*, 868–880.
11. Ramachandran, C.N.; Sathyamurthy, N. Water clusters in a confined nonpolar environment. *Chem. Phys. Lett.* **2005**, *410*, 348–351. [CrossRef]
12. Bloodworth, S.; Sitinova, G.; Alom, S.; Vidal, S.; Bacanu, G.R.; Elliott, S.J.; Light, M.E.; Herniman, J.M.; Langley, G.J.; Levitt, M.H.; et al. First synthesis and characterization of CH_4@C_{60}. *Angew. Chem. Int. Ed.* **2019**, *58*, 5038–5043. [CrossRef] [PubMed]
13. Jaworski, A.; Hedin, N. Local energy decomposition analysis and molecular properties of encapsulated methane in fullerene (CH_4@C_{60}). *Phys. Chem. Chem. Phys.* **2021**, *23*, 21554–21567. [CrossRef]
14. Slanina, Z.; Uhlík, F.; Adamowicz, L. Theoretical predictions of fullerene stabilities. In *Handbook of Fullerene Science and Technology*; Lu X., Akasaka T., Slanina Z., Eds.; Springer: Singapore, 2022; pp. 111–179.
15. Slanina, Z.; François, J.-P.; Kolb, M.; Bakowies, D.; Thiel, W. Calculated relative stabilities of C_{84}. *Fullerene Sci. Technol.* **1993**, *1*, 221–230. [CrossRef]
16. Kikuchi, K.; Nakahara, N.; Honda, M.; Suzuki, S.; Saito, K.; Shiromaru, H.; Yamauchi, K.; Ikemoto, I.; Kuramochi, T.; Hino, S.; et al. Separation, detection and UV/Visible absorption spectra of fullerenes; C_{76}, C_{78} and C_{84}. *Chem. Lett.* **1991**, *20*, 1607–1610. [CrossRef]
17. Bakowies, D.; Kolb, M.; Thiel, W.; Richard, S.; Ahlrichs, R.; Kappes, M.M. Quantum-chemical study of C_{84} fullerene isomers. *Chem. Phys. Lett.* **1992**, *200*, 411–417. [CrossRef]
18. Zhao, Y.; Truhlar, D.G. The M06 suite of density functionals for main group thermochemistry, thermochemical kinetics, noncovalent interactions, excited states, and transition elements: Two new functionals and systematic testing of four M06-class functionals and 12 other functionals. *Theor. Chem. Acc.* **2008**, *120*, 215–241.
19. Ditchfield, R.; Hehre, W.J.; Pople, J.A. Self-consistent molecular-orbital methods. IX. An extended Gaussian-type basis for molecular-orbital studies of organic molecules. *J. Chem. Phys.* **1971**, *54*, 724–728. [CrossRef]
20. Slanina, Z.; Uhlík, F.; Lee, S.-L.; Adamowicz, L.; Akasaka, T.; Nagase, S. Computed stabilities in metallofullerene series: Al@C_{82}, Sc@C_{82}, Y@C_{82}, and La@C_{82}. *Int. J. Quant. Chem.* **2011**, *111*, 2712–2718. [CrossRef]
21. Boys, S.F.; Bernardi, F. The calculation of small molecular interactions by the difference of separate total energies. Some procedures with reduced errors. *Mol. Phys.* **1970**, *19*, 553–566. [CrossRef]
22. Frisch, M.J.; Trucks, G.W.; Schlegel, H.B.; Scuseria, G.E.; Robb, M.A.; Cheeseman, J.R.; Scalmani, G.; Barone, V.; Mennucci, B.; Petersson, G.A.; et al. 2013, Gaussian 09, Rev. C.01, 2016, Gaussian 16, Rev. B.01, Wallingford, CT, Gaussian Inc.
23. Slanina, Z.; Uhlík, F.; Nagase, S.; Akasaka, T.; Adamowicz, L.; Lu, X. A computational characterization of CO@C_{60}. *Fuller. Nanotub. Carbon Nanostructures* **2017**, *25*, 624–629. [CrossRef]

24. Takata, M.; Nishibori, E.; Sakata, M.; Shinohara, H. Charge density level structures of endohedral metallofullerenes determined by synchrotron radiation powder method. *New Diam. Front. Carb. Technol.* **2002**, *12*, 271–286.
25. Hehre, W.J. *A Guide to Molecular Mechanics and Quantum Chemical Calculations*; Wavefunction: Irvine, CA, USA, 2003; p. 435.
26. Jensen, F. *Introduction to Computational Chemistry*; Wiley: Chichester, UK, 2017; p. 319.
27. Campbell, E.K.; Holz, M.; Gerlich, D.; Maier, J.P. Laboratory confirmation of C60+ as the carrier of two diffuse interstellar bands. *Nature* **2015**, *523*, 322–323. [CrossRef]
28. Berné, O.; Tielens, A.G.G.M. Formation of buckminsterfullerene (C_{60}) in interstellar space. *Proc. Natl. Acad. Sci. USA* **2012**, *109*, 401–406. [CrossRef] [PubMed]
29. Berné, O.; Montillaud, J.; Joblin C. Top-down formation of fullerenes in the interstellar medium. *Astronom. Astrophys.* **2015**, *577*, A133-1–A133-9. [CrossRef]
30. Hansen, C.S.; Peeters, E.; Cami, J.; Schmidt, T.W. Open questions on carbon-based molecules in space. *Commun. Chem.* **2022**, *5*, 94-1–94-4. [CrossRef]
31. Slanina, Z.; Fox, K.; Kim, S.J. A computational evaluation of altitude profiles of the equilibrium monomeric-dimeric CO_2 fractions in the atmosphere of Venus. *Thermochim. Acta* **1992**, *200*, 33–39. [CrossRef]
32. Rodríguez-Fortea, A.; Balch, A.L.; Poblet, J.M. Endohedral metallofullerenes: A unique host-guest association. *Chem. Soc. Rev.* **2011**, *40*, 3551–3563. [CrossRef]
33. Basiuk, V. A.; Basiuk, E.V. Noncovalent complexes of I_h-C_{80} fullerene with phthalocyanines. Fuller. Nanotub. *Carbon Nanostructures* **2018**, *26*, 69–75. [CrossRef]
34. Basiuk, V.A.; Tahuilan-Anguiano, D.E. Complexation of free-base and 3d transition metal(II) phthalocyanines with endohedral fullerene $Sc_3N@C_{80}$. *Chem. Phys. Lett.* **2019**, *722*, 146–152. [CrossRef]
35. Li, M.; Zhao, R.; Dang, J.; Zhao, X. Theoretical study on the stabilities, electronic structures, and reaction and formation mechanisms of fullerenes and endohedral metallofullerenes. *Coor. Chem. Rev.* **2022**, *471*, 214762-1–214762-12. [CrossRef]
36. Li, Y.B; Biswas, R.; Kopcha, W.P.; Dubroca, T.; Abella, L.; Sun, Y.; Crichton, R.A.; Rathnam, C.; Yang, L.T.; Yeh, Y.W.; et al. Structurally defined water-soluble metallofullerene derivatives towards biomedical applications. *Angew. Chem. Int. Ed. Engl.* **2023**, *62*, e202211704-1–e202211704-10.